J. Webster (ed.), *Wiley Encyclopedia of Electrical and Electronics Engineering*


# MICROMAGNETICS

Micromagnetic theory has been around for as long as the classical Maxwell's field theory itself (1). However, the modern form of the theory arose from a systematic series of works by William Fuller Brown, Jr., in the late 1950s and early 1960s (2). The theory combines the solution of a subset of Maxwell's equations (those involving magnetic field vectors) with considerations of the material properties of magnetic objects. It is a continuous-medium model of physical quantities and equations that are averaged over small volumes of the material. At the heart of the theory is the postulation of a magnetization vector $\boldsymbol{M}$ of constant magnitude at a given temperature ($|\boldsymbol{M}| = M_s$), defined at each point of a medium, that is equal to the volume average of the atomic magnetic moments of the material. Magnetization equilibrium in a material corresponds to a minimum of the free-energy density of the medium, or equivalently, the vanishing everywhere of the magnetic torque per unit volume acting in the medium. Magnetic moments can be expressed mathematically as magnetic dipoles (doublets of fictitious magnetic charges or poles) or as inaccessible circulating atomic currents (Amperian currents). However, the particular physical origin of the magnetic moments is not germane to micromagnetic theory, as only the magnetization is used to define the free-energy density.

The magnetization $\boldsymbol{M}$ characterizes the sample at a length scale far exceeding that in which atomic processes are important, but small enough so that $\boldsymbol{M}$ adequately represents the magnetization distribution in the body. As a consequence, the volume of definition of $\boldsymbol{M}$ is required to be much smaller than the *exchange length* $L_{ex}$ (3) of the material, which is a distance over which $\boldsymbol{M}$ can, to first order, be considered uniform. In the *ferromagnetic* elements iron, nickel, and cobalt, and their many alloys that have found extensive practical applications, the moments of individual atoms are essentially aligned coherently with those of their neighbors by strong interatomic exchange forces over distances that are many orders of magnitude larger than the lattice constants of the underlying crystal lattice. These materials therefore quite readily satisfy the requirements for the definition of the vector $\boldsymbol{M}$. A similar field averaging is implied in the definition of other field vectors (such as $\boldsymbol{H}$, $\boldsymbol{B}$, and $\boldsymbol{E}$ below). In practice micromagnetic modeling is useful in characterizing the medium at a level of detail that is intermediate between those of quantum-mechanical atomistic models and nonlinear phenomenological models such as the Preisach model (4) that model the medium by mathematical formulas whose parameters are chosen to fit experimental data. Over the years, micromagnetic theory has for the most part been applied to the modeling of magnetic media under *static* or *quasistatic* conditions. These conditions are in effect, respectively, if the magnetic fields inside the sample are constant in time or vary at rates that are much lower than those required for the magnetizing processes in the material to achieve equilibrium. For static methods to apply in conducting magnetic media, eddy currents that are induced in the sample by changing magnetic flux should be negligible.

In addition to the dynamic effects that are described by the time-dependent Maxwell's equations, the atomic moments of magnetic media, by virtue of their intrinsic angular momentum, exhibit a different form of dynamic behavior that is manifested in the inertial response of the moments to applied fields. Thus, unlike an electric dipole, a magnetic moment will not instantly rotate towards an applied field to line up with it. A *free* magnetic moment that is subjected to a constant field will instead *precess* indefinitely about the field direction at a constant angle of inclination to it. Inside a magnetic body, the material constraints imposed

by the body will cause a moment to undergo a more complex *gyromagnetic* motion in response to an applied field. In general the moment will then have to precess about a continually changing total field that is the sum of the externally applied field and internal interaction fields, and will continually lose its kinetic energy to the surrounding crystal lattice, until it becomes aligned with the equilibrium field direction. This energy loss mechanism is referred to as *damping*. The essence of such a damped gyromagnetic motion is conveniently described in micromagnetic calculations by phenomenological equations such as the Landau–Lifshitz equation (5). If damping is sufficiently large in a medium, the energy dissipation may be so rapid that the applied fields quickly equilibrate with the magnetization, before appreciable precession can occur. The magnetization of such media can therefore be treated *quasistatically*. This is not the case for fields that change at rates that are comparable with the damping rate of the magnetization.

Micromagnetic models play significant roles in aiding the design and analysis of modern magnetic devices. Brown's theorems are derived mathematically from well-established experimental observations and thus ensure that the magnetization processes are rigorously modeled. A notable and successful early analytical micromagnetic model was the Stoner–Wohlfarth coherent rotation model (6) that described the magnetization reversal of small uniformly magnetized particles. To obtain accurate results in the overwhelming majority of real-world modeling problems, one needs to apply numerical techniques. This is because real material bodies usually have irregular shapes, and are characterized by complicated microstructural and micromagnetic properties. These give rise to nonuniform magnetization and field distributions in the sample. For example, the Stoner–Wohlfarth model predicts magnetization reversal fields for a particle that are much larger than those measured experimentally, because it ignores incoherent reversal modes, which are natural occurrences in numerical single-particle models (7).

Accurate models represent very cost-effective design tools for the magnetic data storage industry, as they can yield a wealth of information about magnetic devices that may not be accessible by other means, or that would be prohibitively expensive to obtain experimentally. Numerical micromagnetic modeling is a broad subject on which numerous papers have been published over the years. We will not attempt a complete review of these works here, as such a review is worthy of a separate article. For more information the reader may refer to recent articles and books (89–10), which offer extensive reviews of applications of micromagnetic modeling in the design of modern data-storage devices. A variety of older magnetic-materials texts (1112–13) abound, with many examples of early applications of domain and micromagnetic theory.

Advances in computer hardware and software technology over the years have been a major driving force in the now routine simulation of complicated magnetic components in many scientific and engineering groups around the globe. Recently, attempts have been made at developing portable general-purpose micromagnetic software for use in personal computers (14).

The discussion in this article will be limited to micromagnetic theory and modeling of magnetic material under static and quasistatic conditions. Furthermore, we will limit our discussion to ferromagnets. We begin with a review of time-independent Maxwell's equations as they apply to magnetostatic problems. This is followed by a consideration of the main free-energy terms used in micromagnetic modeling. We discuss analytical expressions for these energy terms and their corresponding effective fields, and examine how the interplay of different energies affects the resulting magnetization of the medium. Here too, we compare the different forms of the damped gyromagnetic torque equations commonly used in micromagnetic calculations. Finally, descriptions of two modeling examples (one analytical and the other numerical) are given to illustrate energy minimization procedures. All defining relations are in SI units.

## MAXWELL'S EQUATION FOR MAGNETOSTATIC CONDITIONS

Magnetostatics refers to magnetic field conditions produced by time-independent field sources. Two differential forms of Maxwell's equation that fully describe this situation are

$$\nabla \times \boldsymbol{B} = \mu_0 \boldsymbol{J} = \mu_0(\mathbf{J}_\mathrm{s} + \nabla \times \boldsymbol{M}) = \mu_0(\boldsymbol{J}_\mathrm{s} + \boldsymbol{J}_\mathrm{M}) \qquad (1)$$

and

$$\nabla \cdot \boldsymbol{B} = 0 \qquad (2)$$

where $\boldsymbol{B}$ is the magnetic flux density, $\mu_0$ is the permeability of free space, and $\boldsymbol{J}$ is the total current density, consisting of contributions from external sources $\mathbf{J}_\mathrm{s}$ and fictitious (Amperian current) sources $\mathbf{J}_\mathrm{M} = \nabla \times \boldsymbol{M}$. The magnetic flux density $\boldsymbol{B}$ is related to the magnetic field $\boldsymbol{H}$ by $\boldsymbol{B} = \mu_0 (\boldsymbol{H} + \boldsymbol{M})$. Substituting this into Eq. (1) and Eq. (2) yields

$$\nabla \times \boldsymbol{H} = \boldsymbol{J}_\mathrm{s} \qquad (3)$$

and

$$\nabla \cdot \boldsymbol{H} = -\nabla \cdot \boldsymbol{M} \qquad (4)$$

Equation (2) expresses the fact that the vector $\boldsymbol{B}$ is source-free; Eq. (4) indicates that the source of magnetic field is $-\nabla \cdot \boldsymbol{M}$.

Using the fact that the divergence of the curl of any spatial vector is identically zero, it follows from Eq. (2) that $\boldsymbol{B}$ can be expressed as follows:

$$\boldsymbol{B} = \nabla \times \boldsymbol{A} \qquad (5)$$

where $\boldsymbol{A}$ is an auxiliary vector called the magnetic vector potential. To completely define $\boldsymbol{A}$, its divergence needs to be specified in addition to its curl given by Eq. (5). We will accomplish this, as we seek the solution for $\boldsymbol{B}$, in such a way as to simplify the ensuing transformations of Maxwell's equations. Substituting $\boldsymbol{B}$ from Eq. (5) into Eq. (1) and using the vector relation $\nabla \times \nabla \times \boldsymbol{F} = \nabla (\nabla \cdot \boldsymbol{F})$ - $\nabla^2 \boldsymbol{F}$ (general for any spatial vector $\boldsymbol{F}$) results in

$$\nabla(\nabla \cdot \boldsymbol{A}) - \nabla^2 \boldsymbol{A} = \mu_0 \boldsymbol{J} \qquad (6)$$

With the aim of simplifying the above equation, the divergence of $\boldsymbol{A}$ is now specified as $\nabla \cdot \boldsymbol{A} = 0$. This defines the so-called *Coulomb gauge*. Equation (6) then becomes

$$\nabla^2 \boldsymbol{A} = -\mu_0 \boldsymbol{J} \qquad (7)$$

which is a vector Poisson's equation in $\boldsymbol{A}$. The vector $\boldsymbol{A}$ obtained by solving the above equation can be used together with Eq. (5) to obtain $\boldsymbol{B}$, and subsequently $\boldsymbol{H}$.

It can be shown that Eq. (7) has a unique solution, provided that the requisite *boundary conditions* are satisfied. One set of these conditions stipulates that the tangential components of $\boldsymbol{H}$ and the normal components of $\boldsymbol{B}$ should be continuous at the bounding surfaces of magnetic bodies. A second set of conditions requires the

*regularity at infinity* of components of $\boldsymbol{A}$, meaning that in the limit of very large distances $r$ from field sources, the magnitudes of the components of $\boldsymbol{A}$ and their spatial derivatives should drop off at least as rapidly as $1/r$ and $1/r^2$ respectively.

Outside regions of external current (where $\boldsymbol{J}_s = \boldsymbol{0}$), Eq. (3) transforms to $\nabla \times \boldsymbol{H} = \boldsymbol{0}$ and this implies that $\boldsymbol{H}$ can be found by taking the gradient of a suitable potential function $\varphi$:

$$\boldsymbol{H} = -\nabla\phi \tag{8}$$

Combining this equation with Eq. (4) results in

$$\nabla^2\varphi = \nabla\cdot\boldsymbol{M} \tag{9}$$

which is a scalar Poisson's equation in $\varphi$. Boundary conditions similar to those imposed on Eq. (7) are required for Eq. (9) to yield a unique solution. The conditions of regularity at infinity in this case applies to the potential function. A detailed review of different solution techniques for magnetostatic problems by solving Eq. (8) can be found in Ref. 15. The integration of Eq. (9) and the subsequent application of Eq. (8) yields the expression for the total field at a field point:

$$\boldsymbol{H} = -\frac{1}{4\pi}\int \frac{\nabla\cdot\boldsymbol{M}}{r^2}\hat{\boldsymbol{r}}\, dv + \frac{1}{4\pi}\int \frac{\boldsymbol{M}\cdot\hat{\boldsymbol{n}}}{r^2}\hat{\boldsymbol{r}}\, dS \tag{10}$$

which, by analogy to electrostatic fields, portrays $\boldsymbol{H}$ as composed of contributions from volume "magnetic charges" $-\nabla\cdot\boldsymbol{M}$ and surface "charges" $\boldsymbol{M}\cdot\hat{n}$ on boundary surfaces of the region ($\boldsymbol{r}$ is the coordinate vector drawn from source to field points, $\hat{r}$ is its corresponding unit vector, and $\hat{n}$ is an outward unit normal to a surface).

## FREE-ENERGY DENSITIES AND EFFECTIVE FIELDS

The contents of this and the following section are a cursory treatment of material that can be found elsewhere in greater detail and rigor (Ref. 2, Chaps. 6, 7).

The equilibrium magnetization states arrived at in micromagnetic calculations correspond to local minima of the free energy of the system. In this section we examine more closely the various energy terms that play important roles in determining the magnetic behavior of media. We consider the *Zeeman*, the *magnetocrystalline anisotropy*, and the *exchange* energy term, which are usually the most significant energies in ferromagnetic materials. Following the treatment of energies, the notion of *effective magnetic fields* inside a magnetic medium corresponding to the energy terms is given. This leads to the derivation of the equivalence of the condition of an energy minimum to the vanishing of the torque per unit volume at every point in the material. Other possible energy terms not considered here (for example, surface-anisotropic and magnetostrictive energies) may be included in micromagnetic calculations when needed, following the framework outlined below.

### Zeeman energy.

*External field energy. Magnetostatic energy.* The energy of a magnetic moment in the presence of a magnetic field is called the *Zeeman energy*. The moment experiences a rotating torque that tends to align it with the field so as to minimize this energy. The Zeeman energy density at a point of the magnetic medium is

given by the expression

$$W_Z = -\boldsymbol{M}\cdot\boldsymbol{B} = -\mu_0\boldsymbol{M}\cdot\boldsymbol{H} - \mu_0 M^2 \tag{11}$$

From the micromagnetic assumption of a constant $\boldsymbol{M}$, it follows that the term $\mu_0 M^2$ in Eq. (11) is constant and positive. We may drop this term by shifting the energy reference value by this amount to obtain

$$W_Z = -\mu_0\boldsymbol{M}\cdot\boldsymbol{H} = -\mu_0\boldsymbol{M}\cdot(\boldsymbol{H}_d + \boldsymbol{H}_o) \tag{12}$$

In the above equation, $\boldsymbol{H}$ is the total applied field acting at the point where the energy density is being evaluated, and consists of the self-demagnetizing field $\boldsymbol{H}_d$ of the medium and the field $\boldsymbol{H}_0$ from external sources. The self-demagnetization term and the other external fields emanating from sources given by $-\nabla\cdot\boldsymbol{M}$ [see Eq. (4)] are collectively referred to as *magnetostatic* energy terms.

The total Zeeman energy $E_Z$ of the medium of volume $V$ can be found by taking the volume integral of Eq. (12) over the region of space occupied by the medium:

$$E_Z = -\left(\frac{\mu_0}{2}\int_V \boldsymbol{M}\cdot\boldsymbol{H}_d\,dv - \mu_0\int_V \boldsymbol{M}\cdot\boldsymbol{H}\,dv\right) \tag{13}$$

The division by 2 of the self-demagnetizing energy in the above integration is needed to prevent double counting of the integrand $-\mu_0\boldsymbol{M}\cdot\boldsymbol{H}_d$, which represents the mutual interaction energy between field and source points. The external field energy per unit volume of a uniformly magnetized body is equal to $-\mu_0\boldsymbol{M}\cdot\langle\boldsymbol{H}\rangle$, where $\langle\boldsymbol{H}\rangle = (1/V)\int\boldsymbol{H}\,dv$ is the volume average of the external field over the object.

*Reciprocity. Pole avoidance.* A collection of theorems that play useful roles in both the development of micromagnetic theory and its use in the solution of practical problems comprises the *reciprocity* theorems. One version of it relating the magnetization of interacting bodies with the fields they produce takes the form

$$\int \boldsymbol{H}_i\cdot\boldsymbol{M}_j\,dv = -\int \boldsymbol{H}_i\cdot\boldsymbol{H}_j\,dv = \int \boldsymbol{M}_i\cdot\boldsymbol{H}_j\,dv \tag{14}$$

where $\boldsymbol{H}_i$ is the field produced by magnetization $\boldsymbol{M}_i$ at the location of magnetization $\boldsymbol{M}_j$, whose field in turn at the location of $\boldsymbol{M}_i$ is $\boldsymbol{H}_j$. The integrals are taken over all space. The theorem indicates that either of the integrals on both sides of Eq. (14) may be substituted for the other in expressions. This often provides powerful simplifications in the solution of problems involving interacting bodies. Thus, the solution of a problem whose formulation involves one of the integrals of Eq. (14) directly may at first prove unwieldy. However, the solution may greatly simplify if the integral is swapped with one of its equivalents from Eq. (14). Such a technique is utilized to great effect in calculating the readback signals of read heads in magnetic recording systems (16).

Equation (14) is applicable regardless of the relative locations of the interacting bodies. As a special case, the bodies may even be coincident. This results in the following corollary of Eq. (14):

$$\int \boldsymbol{H}\cdot\boldsymbol{M}\,dv = -\int H^2\,dv \tag{15}$$

Using this result, the expression for the self-demagnetizing energy of a body can be rewritten as follows:

$$E_{\mathrm{d}} = -\frac{\mu_0}{2} \int \boldsymbol{M} \cdot \boldsymbol{H}_{\mathrm{d}} \, dv = \frac{\mu_0}{2} \int H_{\mathrm{d}}^2 \, dv \tag{16}$$

Since the integrand in the above expression is always positive, the energy is minimized for $\mathbf{H}_{\mathrm{d}} = \mathbf{0}$ if possible. Equation (16) expresses the *pole avoidance* tendencies of the medium, whence the magnetization distribution within the body strives to assume a configuration that eliminates the magnetic poles that are the source of $\boldsymbol{H}_{\mathrm{d}}$, so as to minimize the self-demagnetizing energy of the sample. This property will be recalled later on in this article in discussions of magnetization distributions in samples.

**Magnetocrystalline anisotropy energy.** Anisotropies in the crystal symmetry of magnetic materials can lead to tendencies of the magnetization vectors to orient favorably in certain crystallographic directions (easy axes) as opposed to other directions (hard axes). The energy associated with this behavior is called the magnetocrystalline or magnetic anisotropy energy and is a function of the orientation of the magnetization vector. Magnetic anisotropy energies are customarily modeled as the leading terms in the power series expansion of the energies in the angular coordinate coefficients of the magnetization relative to crystal lattice cells. Two commonly considered magnetocrystalline anisotropies in micromagnetic modeling are *uniaxial* and *cubic* anisotropies. We now examine these separately.

*Uniaxial anisotropy.* This anisotropy is typically characterized by the presence of an easy axis that is oriented normal to a *hard plane*. This is illustrated in Fig. 1 for the ferromagnetic element cobalt, which exhibits this type of anisotropy. Cobalt has a hexagonal crystal lattice. The easy axis at room temperature is parallel to the crystal $c$ axis, which is normal to the basal plane of the hexagonal unit cell. In the figure, the magnetization vector makes an angle $\theta$ with the $c$ axis. The energy increases from a minimum value as $\theta$ is varied from $0^\circ$ and attains a maximum at $\theta = 90^\circ$. The free-energy-density expansion is usually carried out in powers of $\sin^2 \theta$, resulting in a leading term of the form

$$W_{\mathrm{k}} = K_{\mathrm{u}} \, \sin^2 \theta \tag{17}$$

where $K_{\mathrm{u}} > 0$ is the uniaxial anisotropy constant. In materials having negative $K_{\mathrm{u}}$, the energy density attains its maximum and minimum at $\theta = 0^\circ$ and $\theta = 90^\circ$ respectively. Such media are characterized by a hard axis that is perpendicular to an *easy plane*.

*Cubic anisotropy.* Elements such as iron and nickel that have cubic crystal lattices also exhibit cubic magnetic anisotropies. These materials have three equivalent mutually perpendicular easy axes coinciding with the three directions of the crystallographic basis vectors describing the cubic unit cell ($\langle 100 \rangle$ directions). The leading term in the power series expansion of the energy density is usually taken in the form

$$W_{\mathrm{k}} = K_{\mathrm{c}}(\alpha^2\beta^2 + \beta^2\delta^2 + \delta^2\alpha^2) \tag{18}$$

where $K_{\mathrm{c}} > 0$ is the cubic anisotropy constant and $\alpha$, $\beta$, and $\delta$ are the direction cosines of the magnetization vector with respect to the three crystalline directions. The form of Eq. (18) is consistent with the cubic symmetry of the material: It is devoid of odd powers of the direction cosines and is invariant to the interchange of any two direction cosines. The total magnetocrystalline anisotropy energy of a magnetic medium is given by

$$E_{\mathrm{k}} = \int W_{\mathrm{k}} \, dv \tag{19}$$

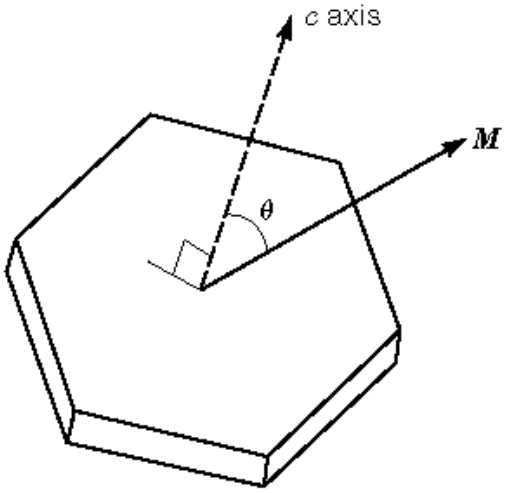


**Fig. 1.** Uniaxial magnetic anisotropy in a hexagonal cobalt platelet. The *c* axis is the *easy axis*, and the basal plane of the platelet is the *hard plane*.

In some cubic materials it is possible to express the magnetic anisotropy similarly by Eq. (18), but with an anisotropy constant that is negative. Such media are characterized by four easy directions along the diagonals of the cubic unit cell (⟨111⟩ directions).

**Exchange energy.** A short-range ordering of magnetization exists in ferromagnetic bodies due to quantum-mechanical ferromagnetic exchange coupling forces between atomic spins in the material (17). In the absence of other forces the exchange promotes a uniform direction of the magnetization across the sample. The Heisenberg exchange interaction energy between two atomic spins is given by

$$W_{\mathrm{x}} = -2J\boldsymbol{S}_i \cdot \boldsymbol{S}_j \tag{20}$$

where $\boldsymbol{S}_i$ is the net spin angular momentum of the $i$th atom and $J$ is the exchange integral.

The following form of the total exchange energy of the sample is almost exclusively adopted in calculations:

$$E_{\mathrm{x}} = -\int A\hat{\boldsymbol{m}} \cdot \nabla^2 \hat{\boldsymbol{m}}\, dv \tag{21}$$

where $A(r) > 0$, a function of position, is the phenomenological exchange parameter of the material and $\hat{m}$ is the unit magnetization vector. It should be noted that in spite of its near-universal use, Eq. (21) is derived from Eq. (20) by considering a cubic lattice of atomic spins that can be treated as a continuous function of position in regions where the magnetization is uniform or very nearly so (Ref. 2, Chaps. 6, 7). In this case, explicit expressions relating the exchange constant $A$ to the cubic lattice constants are found. Because Eq. (21) is derived for conditions of small angular deviations of neighboring spins, it is often referred to as the *small-angle* expression of exchange energy, and strictly speaking is no longer accurate for large angles, although heed is seldom paid to this fact in practice. The continuity of magnetization implicit in the derivation of Eq. (21) also leads to predictions of unphysical infinite exchange energies in regions of magnetization singularities such as the cores of magnetization vortex structures.

**Effective fields.** The total energy of a magnetic specimen is obtained by summing the terms given above to obtain

$$E = E_Z + E_k + E_x = \int (\mu_0 \boldsymbol{M} \cdot \mathbf{H} - \tfrac{1}{2}\mu_0 \boldsymbol{M} \cdot \boldsymbol{H}_d + W_k - A\hat{\mathbf{m}} \cdot \nabla^2 \hat{\boldsymbol{m}})\, dv \qquad (22)$$

In the solution of micromagnetic problems, a magnetization distribution corresponding to a stable local minimum of the energy of the sample is sought. In accord with variational calculus, at equilibrium, the first variation $\delta E$ of the energy must vanish, and for stability, the second variation $\delta^2 E$ must be positive. Micromagnetic theory imposes the additional constraint that the magnetization vector of each point in the medium must remain fixed in magnitude ($|\boldsymbol{M}| = M_s$). The variation of the total energy [Eq. (22)] can be expressed as follows (the reader is referred to Ref. 2, Chaps. 6, 7, for a full derivation):

$$\delta E = \int \frac{\partial W}{\partial \boldsymbol{M}} \cdot \delta \boldsymbol{M}\, dv = -\mu_0 \int \mathbf{H}_{\text{eff}} \cdot \delta \boldsymbol{M}\, dv \qquad (23)$$

where

$$\boldsymbol{H}_{\text{eff}} = \boldsymbol{H} + \boldsymbol{H}_d + \boldsymbol{H}_k + \mathbf{H}_x = \boldsymbol{H} + \boldsymbol{H}_d - \frac{1}{\mu_0 M_s}\frac{\partial W_k}{\partial \boldsymbol{M}} + \frac{1}{2\mu_0 M_s}\nabla \cdot (A \nabla \hat{\boldsymbol{m}}) \qquad (24)$$

has the dimensions of a magnetic field, and is called the *effective field* inside the medium. As might be expected, the external and magnetostatic field terms appear explicitly in Eq. (24). The resulting expressions for $\boldsymbol{H}_k$ and $\boldsymbol{H}_x$ depend on the respective forms of the magnetic anisotropy energy $W_k$ and the exchange function $A$. Once $\boldsymbol{H}_{\text{eff}}$ has been obtained, the energy density at each point of the sample may be expressed in its *Zeeman* form, $-\mu_0 \boldsymbol{M} \cdot \boldsymbol{H}_{\text{eff}}$, so called because of its similarity to Eq. (12).

Since $\boldsymbol{M}$ must remain fixed in magnitude, the variation $\delta \boldsymbol{M}$ can only occur through the rotation of the magnetization vector. Thus we can write

$$\delta \boldsymbol{M} = \delta \boldsymbol{\theta} \times \boldsymbol{M} \qquad (25)$$

where $\delta\theta = \hat{e}\ \delta\theta$ represents a rotation through angle $\delta\theta$ about an arbitrary direction pointed to by the unit vector $\hat{e}$. Since the magnitude of $\boldsymbol{M}$ should remain fixed, only components of $\delta\theta$ that are perpendicular to $\boldsymbol{M}$ will be effective in the cross product of Eq. (25). After substituting Eq. (25) into Eq. (23) and carrying out the transformations $-\boldsymbol{H}_{\text{eff}} \cdot \delta \boldsymbol{M} = -\boldsymbol{H}_{\text{eff}} \cdot \delta\theta \times \boldsymbol{M} = -\boldsymbol{M} \times \boldsymbol{H}_{\text{eff}} \cdot \delta\theta$, we have

$$\delta E = -\int \boldsymbol{M} \times \boldsymbol{H}_{\text{eff}} \cdot \delta \boldsymbol{\theta}\, dv \qquad (26)$$

As the rotation $\delta\theta$ can be chosen arbitrarily in the material, the equilibrium condition $\delta E = 0$ implies from the above that

$$\boldsymbol{M} \times \boldsymbol{H}_{\text{eff}} = \mathbf{0} \qquad (27)$$

The cross product $\boldsymbol{M} \times \boldsymbol{H}_{\text{eff}}$ represents the torque per unit volume due to the total field (external plus internal effective fields) acting on the sample. Thus the local energy minimum condition is equivalent to the vanishing of the torque at every point of the medium.

The energy-minimum state is still to be subjected to further analysis to ensure that it is a stable one. Only in a few ideal cases (see for example the Stoner-Wohlfarth model below) it is possible to conduct this test analytically by evaluating the second-order energy variation directly. In practical numerical calculations, this check is usually carried out by slightly perturbing the equilibrium magnetization and ascertaining that the sample then experiences a restoring force that reestablishes the equilibrium condition.

*Micromagnetic magnetization structures. Domains. Domain walls.* Physical magnetizing processes in magnetic materials are in general highly nonlinear and hysteretic. The magnetic states that arise in a sample depend on the relative magnitudes and interplay of the various energy components discussed above. The effect of each term manifests itself on how that term affects the magnetization distribution to minimize its contribution to the total energy. Thus, as seen from Eq. (11), an external field will tend to rotate the magnetization vector at each point to line up with it, so as to minimize the external field energy. Indeed this is what every field component tries to do if magnetic interactions are viewed solely in terms of effective fields. Magnetostatic interactions encourage the formation of magnetization distributions that are free from uncompensated magnetic charges, as suggested by the pole avoidance relation, Eq. (15). One consequence of this is that magnetization vectors tend to rotate away from the edges of samples, and instead try to lie parallel to them.

Magnetostatic energy is also minimized by a magnetic *vortex* as shown in Fig. 2(a). Magnetocrystalline anisotropy promotes the formation of large regions of uniform magnetization called *domains* along magnetically easy directions, and exchange interaction promotes uniform short-range ordering of magnetization.

Figure 2(b) illustrates schematically some possible magnetic structures that can arise in the plane of a thin rectangular film sample of a cubic crystal such as iron, if the sides of the rectangle are parallel to the easy ($\langle 100 \rangle$) directions. The magnetic anisotropy promotes the formation of the domains; the magnetostatic interactions, on the other hand, cause the magnetization to be oriented parallel to the plane of the sample and to its sides and to form so-called *closure domains* at the ends of the sample (domains I and IV in the figure). The domains are separated by *domain walls*. These are portrayed as straight lines in Fig. 2, to correspond to the scale of the problem. They usually have more structure to them, as we will examine shortly. The domain walls in the figure are oriented in such a way so that the net charge at the walls is zero according to the pole-avoidance principle.

The magnetization changes rapidly in direction inside a domain wall through an angle given by the difference in the direction of the domains bordering the wall. As suggested by Fig. 2, the domain-wall width $L_{\text{w}}$ is usually much smaller than the sizes of domains. Domain walls are classified according to the angle between the domains they separate and according to their magnetic structures. Thus wall $A$ of Fig. 2 is a 180° wall, and wall $B$ is a 90° wall. The details of the wall structure for the two simplest domain wall structures [the *Bloch wall* and the *Néel wall* (17)] are shown in Fig. 3 for a 180° wall. In a Bloch wall, the magnetization rotates uniformly in directions parallel to the wall plane (the $z$–$y$ plane in the figure), while for the Néel wall the rotation is perpendicular to the wall plane (the $x$–$z$ plane in the figure). Exchange interactions promote the widening of the domain wall as this makes the variation of magnetization more gradual by decreasing the angle between the magnetization of neighboring points in moving across the wall [along $x$ in Fig. 3(a)]. Magnetic anisotropy, by contrast, encourages narrower walls in order to minimize the amount of the deviation of the magnetization from easy-axis directions. The final wall width is the result of a compromise between these two competing effects. In the bulk of the material, Bloch walls between domains are energetically more favorable than Néel walls. Néel walls, however, are more prevalent in thin-film media, as Bloch walls would produce surface charges at the film surfaces that would increase the self-demagnetizing energy of the wall. More complicated wall structures such as asymmetric Bloch walls and *cross-tie walls* (see, e.g., Ref. 11, Chap. 18, and Ref. 18) are also possible.

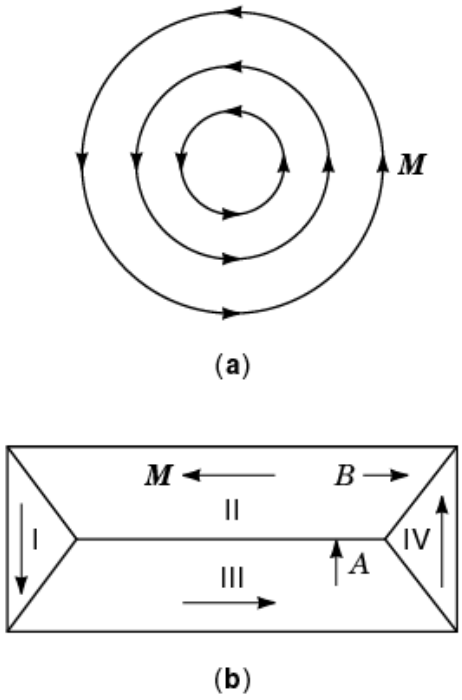


**Fig. 2.** (a) Planar magnetization vortex structure, (b) illustration of magnetic domains in a thin-film sample. Regions I, II, III, and IV are uniformly magnetized magnetic domain regions (the end domains III are IV are called *closure domains*); $A$ and $B$ are 180° and 90° domain walls respectively.

*Single-Domain Particles. Demagnetizing Factors.* The magnetic structure of a ferromagnetic body at equilibrium is one composed of many domains that are separated by domain walls. A ferromagnetic particle that is smaller in size than the width of a domain wall, will be unable to sustain domain walls and will therefore become essentially *single-domain*.

In general, the demagnetizing field inside a single-domain particle is nonuniform even though its magnetization is uniform. This demagnetizing field is equal to $\boldsymbol{H}_{\mathrm{d}}{}' = -\boldsymbol{N}\,(r) \cdot \boldsymbol{M}$, where $\boldsymbol{N}(r)$ is a point-to-point demagnetizing tensor that can be represented mathematically by a $3 \times 3$ matrix. The volume-average demagnetizing field found by averaging $\boldsymbol{H}'_{\mathrm{d}}$ over the volume of the particle is equal to $\boldsymbol{H}_{\mathrm{d}} = -\boldsymbol{N} \cdot \boldsymbol{M}$, where the demagnetizing tensor $\boldsymbol{N}$ in general is different from $\boldsymbol{N}(r)$. For regularly shaped particles, if $\boldsymbol{N}$ is referred to the particle principal axes ($xyz$, say), then it transforms into a diagonal matrix, whose diagonal elements $N_x$, $N_y$, $N_z$ are called *demagnetizing factors*, are positive, and obey the condition (in SI units)

$$N_x + N_y + N_z = 1 \tag{28}$$

The demagnetizing field in this case can be expressed as

$$\boldsymbol{H}_{\mathrm{d}} = -(N_x M_x \hat{\boldsymbol{\imath}} + N_y M_y \hat{\boldsymbol{\jmath}} + N_z M_z \hat{\boldsymbol{k}}) \tag{29}$$

where $M_x$, $M_y$, $M_z$ are the magnetization components along the coordinate axes, and $\hat{\imath}, \hat{\jmath}, \hat{k}$ are the coordinate unit vectors.

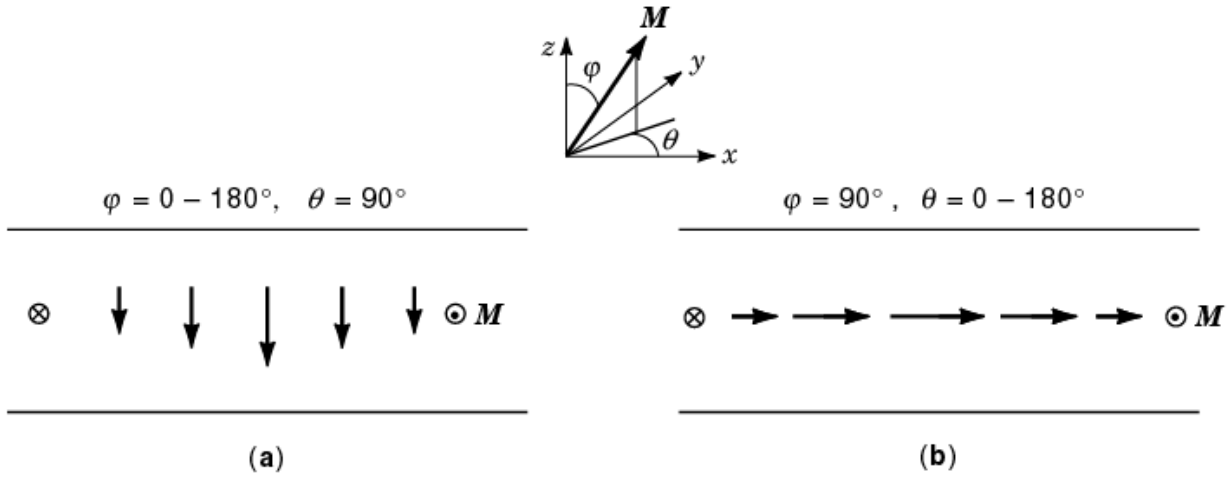


**Fig. 3.** Schematic of magnetization rotation in (a) Bloch and (b) Néel domain walls.

From the above relation it is obvious that the demagnetizing factor along a given principal axis is simply the magnitude of the field per unit magnetization when the particle is magnetized along that axis. The sources of this field are the induced surface charges at the ends of the particle along the axis. Thus, one may expect on physical grounds that the particle will have smaller demagnetizing factors along axes where it is longer, and larger factors along axes where it is shorter, creating a *shape anisotropy* in the particle. In the absence of other anisotropies, the axes that correspond to the smaller demagnetizing factors define easy magnetization axes for the particle. Only for particles that have ellipsoidal shapes (Fig. 4) can the magnetization and demagnetizing field be both uniform inside the particle. The demagnetizing field of an ellipsoidal particle is independent of its volume. The two demagnetizing tensors $\boldsymbol{N}(r)$ and $\boldsymbol{N}$ are equal for ellipsoids. From Eq. (28) and shape symmetry considerations, one may draw the following conclusions regarding the demagnetizing factors for certain ellipsoidal shapes: (1) spheroid ($a = b \neq c$), $N_x = N_y \neq N_z$; (2) sphere ($a = b = c$), $N_x = N_y = N_z = 1/3$; (3) infinitely long cylinder along z axis ($a = b$, $c = \infty$), $N_x = N_y = 1/2$, $N_z = 0$; (4) oblate (pancake-shaped) particle ($a = b \gg c$), $N_x = N_y = 0$, $N_z = 1$). The reader can find a complete discussion of the general properties of demagnetizing tensors for both regularly and irregularly shaped bodies in Ref. 19.

*Gyromagnetic motions of magnetization.* The magnetization vector $\boldsymbol{M}$ has an angular momentum per unit volume $\boldsymbol{L}$ associated with it that is defined as follows (Ref. 11, Chap. 2):

$$\boldsymbol{M} = -\frac{g\mu_0|e|}{2m_e}\boldsymbol{L} = -\gamma_0\boldsymbol{L} \tag{30}$$

where $|e|/m_e$ is the electronic charge–mass ratio, $\gamma_0$ is the gyromagnetic constant, and $g$ is the gyromagnetic ratio, which is equal to 1 or 2 according as the source of magnetization of the material is attributable to spin or to orbital electronic motion. According to classical Newtonian mechanics, the rate of change of the angular momentum per unit volume in response to an applied field $\boldsymbol{H}$ is equal the torque per unit volume acting on $\boldsymbol{M}$, that is, $d\boldsymbol{L}/dt = -\boldsymbol{M} \times \boldsymbol{H}$, so that $d\boldsymbol{M}/dt = -\gamma_0\boldsymbol{M} \times \boldsymbol{H}$. In view of the constancy requirement on the magnitude of $\boldsymbol{M}$, only components of $\boldsymbol{H}$ that are perpendicular to $\boldsymbol{M}$ are effective in the cross product. Thus, this relation describes the precession of $\boldsymbol{M}$ about $\boldsymbol{H}$ at angular velocity $\omega = \gamma_0 H$.

Loss mechanisms in the medium cause the precessing magnetization to progressively line up with the applied field and the torque to vanish. This energy loss process is called *damping*. Two most commonly used

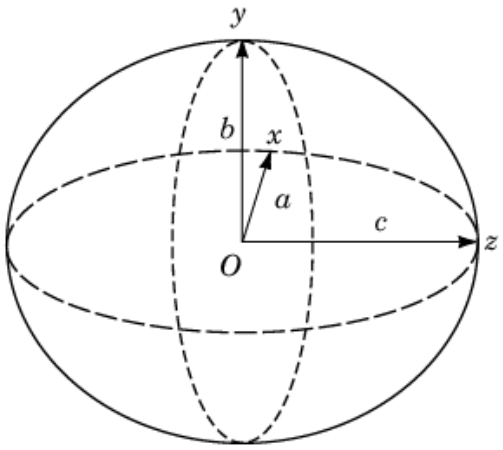


**Fig. 4.** Geometry of ellipsoidal particle.

phenomenological equations to describe such damped gyromagnetic motion in calculations are the Landau–Lifshitz (*LL*) equation in its original form and with a Gilbert damping term included (5). Both equations can be expressed as follows:

$$\frac{d\boldsymbol{M}}{dt} = \gamma \boldsymbol{M} \times \boldsymbol{H} - \beta \frac{\boldsymbol{M} \times (\boldsymbol{M} \times \boldsymbol{H})}{M} \tag{31}$$

where the first term on the right is the precession term and the second is the damping term, $\gamma$ is the precession factor, and $\beta$ is a phenomenological damping factor. Both factors are constant in the original *LL* form ($\gamma = \gamma_0$). In the Gilbert form $\gamma = \gamma_0/(1 + \alpha^2{}_{\mathrm{G}})$ and $\beta = \alpha_{\mathrm{G}}\gamma_0/(1 + \alpha^2{}_{\mathrm{G}})$, where $\alpha_{\mathrm{G}}$ is the Gilbert damping factor. Inside the medium, $\boldsymbol{H}$ is equal to the effective field $\boldsymbol{H}_{\mathrm{eff}}$. The Gilbert form follows from a derivation (20) in which the effective field is augmented by a velocity-dependent Rayleigh friction term in Eq. (30), with $\boldsymbol{M}$ treated as a generalized coordinate and $\boldsymbol{H}$ as a generalized force. In the older *LL* equation, the precession and damping are decoupled. This implies that for an isolated magnetic moment, the angular velocity of precession will be independent of the damping factor, and the relaxation time will be inversely proportional to the damping constant. Such an outcome is at odds with intuitive physical reasoning. The precession and damping terms are interrelated in the Gilbert form. This results in an angular velocity of precession of an isolated moment that is inversely proportional to damping, a physically more realistic behavior.

Because these equations mimic actual physical behavior, they are widely used in modeling situations when it is important to understand the time evolution of the magnetization between equilibrium states.

## ENERGY MINIMIZATION EXAMPLES

Two examples of energy minimization procedures in solving micromagnetic problems will be given in this section. The first example will be a brief treatment of the analytical *Stoner–Wohlfarth model* for ellipsoidal single-domain particles. We will skip most of the details and will highlight the main points of the model. Our second example considers in some detail the numerical techniques involved in simulating the magnetization of a thin-film sample that is subjected to an applied field.

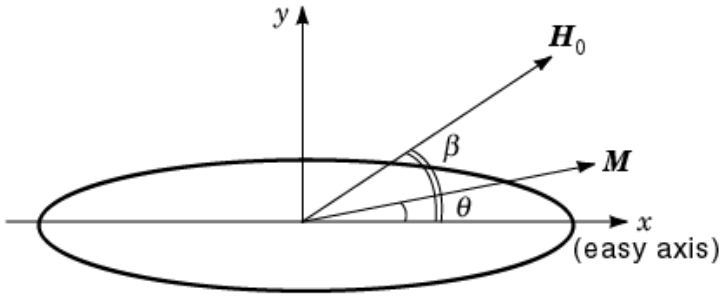


**Fig. 5.** Geometry of Stoner–Wohlfarth model.

**The Stoner–Wohlfarth model.** This model described in the landmark paper by Stoner and Wohlfarth (6) represents the first realistic physical micromagnetic model of a magnetic body. The analysis is carried out for an ellipsoidal single-domain particle. Consider the single-domain prolate spheroid shown in Fig. 5. The $x$ axis is the easy direction of the magnetic anisotropy determined by the shape of the particle. Also shown in the figure are definitions of the angular orientations of the external field $\boldsymbol{H}_0$ and magnetization $\boldsymbol{M}$ relative to the easy axis. The self-demagnetizing energy density due to the shape anisotropy of the particle can be shown (after appropriate shifting of energy reference) to be equal to $1/2\mu_0 M^2{}_\mathrm{s}\,(N_y - N_x)\sin^2\theta$. Let us further assume, for simplicity, that the particle is characterized by a uniaxial magnetic anisotropy given by Eq. (17) whose easy axis coincides which the $x$ axis. Then, since this expression follows the same angular dependence as the shape-anisotropy energy, both terms may be combined into a single term in energy expressions.

We are interested in finding the equilibrium orientation of the magnetization in response to the field $\boldsymbol{H}_0$. By symmetry $\boldsymbol{M}$ must lie in the plane of $\boldsymbol{H}_0$ and the $x$ axis. The external-field energy density from Eq. (11) is given by

$$\begin{aligned} E_\mathrm{ext} &= -\mu_0 \boldsymbol{M}\cdot\boldsymbol{H} = -\mu_0 M_\mathrm{s}(H_0 \sin\beta \sin\theta + H_0 \cos\beta \cos\theta) \\ &= -\mu_0 M_\mathrm{s}(H_y \sin\theta + H_x \cos\theta) \end{aligned} \tag{32}$$

where $H_x$ and $H_y$ are the $x$ and $y$ components of the external field. Thus, the free-energy density of the particle, consisting of anisotropy and external-field terms, is equal to

$$E = -\mu_0 M_\mathrm{s}(H_y \sin\theta + H_x \cos\theta) + K_\mathrm{eff} \sin^2\theta \tag{33}$$

where $K_\mathrm{eff} = K_\mathrm{u} + 1/2\ \mu_0 M^2{}_\mathrm{s}\,(N_y - N_x)$ is the effective anisotropy constant, incorporating shape and magnetocrystalline anisotropies. The exchange energy plays no role in this model, since the particle is constrained to be always uniformly magnetized.

For equilibrium, the derivative of Eq. (33) with respect to $\theta$ must vanish, resulting in

$$\frac{1}{\mu_0 M_\mathrm{s}}\frac{dE}{d\theta} = H_x \sin\theta - H_y \cos\theta - H_\mathrm{k} \sin\theta \cos\theta = 0 \tag{34}$$

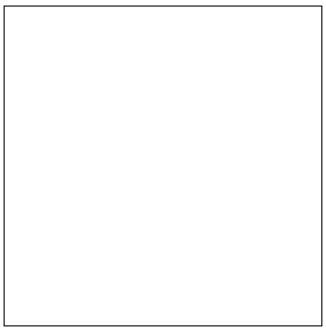

**Fig. 6.** Illustration of magnetization curves predicted by the Stoner–Wohlfarth model for a single-domain particle: (a) family of magnetization curves as a function of field angle $\beta$; (b) magnetization curve for $\beta = 60^\circ$; (c) coercive field $H_c$ and critical field $H_{cr}$ as functions of field angle.

where $H_k = 2K_{eff}/(\mu_0 M_s)$ is called the *anisotropy field*. For stability, the second derivative must be greater than zero; thus

$$\frac{1}{\mu_0 M_s}\frac{d^2E}{d\theta^2} = H_x \cos\theta + H_y \sin\theta + H_k(\sin^2\theta - \cos^2\theta) > 0 \qquad (35)$$

A more detailed analysis reveals the following two salient features of the model: (1) sections of magnetization curves with positive slopes represent stable states, and (2) the particle has a field-dependent energy profile, with respect to angle $\theta$, having two local minima at zero field along the easy axis, that is, at $\theta = 0^\circ$ and $\theta = 180^\circ$. An increasing applied field causes the local minimum it makes an acute angle with to deepen, and the second minimum to become shallower until it disappears altogether at some *critical (switching) field*, $H_{cr}$. The system then falls into the one remaining energy well. If the energy state of the particle was originally in the now vanished well, then this transition into the new state represents an *irreversible* magnetization reversal. If the applied field does not exceed the critical value, then the magnetization process will be completely *reversible*.

These considerations lead to the predicted magnetization curves for the particle that are shown in Fig. 6(a) for four different orientations of the external field. The $60^\circ$ curve, which is plotted separately in Fig. 6(b), shows that the coercive field $H_c$ and switching field $H_{cr}$ for the particle are unequal. They are equal along the particle $M$–$H$ curves from $0^\circ$ up to $\beta = 45^\circ$, and diverge thereafter [Fig. 6(c)]. The critical fields for $\beta = 0^\circ$ and $\beta = 90^\circ$ are both equal to the anisotropy field $H_k$.

The second derivative of the energy vanishes when the applied field attains a critical value. Setting $d^2E/d\theta^2$ to zero in Eq. (35) and solving the ensuing equation simultaneously with Eq. (34) results in the following *astroid* equation, which the critical fields obey:

$$H_x^{2/3} + H_y^{2/3} = (H_k)^{2/3} \qquad (36)$$

An elegant geometric construction for determining the magnetization direction, based on above astroid equation, has been described (21). This technique is illustrated in Fig. 7.

**Numerical micromagnetic modeling of thin-film media.** We now consider the numerical modeling of a thin magnetic film (Fig. 8), using a solution method that seeks the satisfaction of the equilibrium torque condition [Eq. (27)]. This example gives a flavor of the typical considerations that come into play in the rigorous micromagnetic modeling of magnetic components used in the design of real magnetic devices. The highly

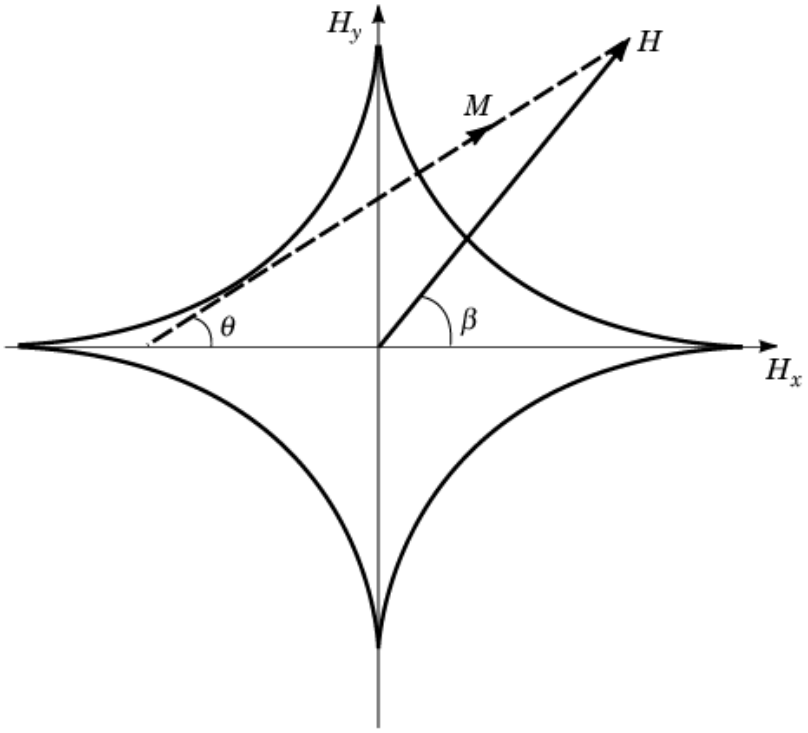


**Fig. 7.** Geometric determination of magnetization direction predicted by the Stoner–Wohlfarth model, using the astroid defined by Eq. (35) of the text [after Prutton (21)]. The field $\boldsymbol{H}$ is drawn from the origin $\boldsymbol{O}$. The magnetization $\boldsymbol{M}$ is parallel to the tangent to the astroid drawn from the tip of the vector $\boldsymbol{H}$.

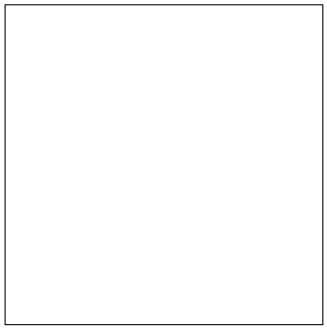

**Fig. 8.** Numerical example: (a) division of thin-film medium; (b) close-up of a volume element.

nonlinear nature of the problem necessitates the use of numerical iteration techniques. In the discussion we will occasionally digress from the narration of the example at hand, to review briefly other general observations for a particular issue being examined.

The main objective of our example is to calculate the equilibrium magnetization distribution $\boldsymbol{M}(r)$ in the sample in response to an external field $\boldsymbol{H}_0(r)$ that may or may not be uniform over the sample. The magnetization is assumed to be constant through the thickness of the film (the $z$ direction), that is, $\boldsymbol{M} = \boldsymbol{M}(x,$

$y$). Magnetic anisotropy directions are assumed to vary from point to point in the sample. We consider the case of local uniaxial anisotropy, which can be described by Eq. (17). We assume further that the sample is materially homogeneous, meaning that both the anisotropy factor $K$ and the exchange factor $A$ are constant functions of coordinates. The following inputs are assumed known beforehand: (1) the values of $A$ and $K$, (2) the initial magnetization distribution inside the sample, and (3) the distribution of magnetic easy-axis orientations among elements.

We first discretize the sample by dividing it into a regular *monolayer* $n \times m$ array of identical volume elements having square cross sections of size $h$ in the film plane, as shown in Fig. 8. The total number of elements is $N = nm$. Each element is assumed to be single-domain with a fixed magnetization vector $\boldsymbol{M}_i$, and is characterized by a magnetocrystalline anisotropy unit vector $\hat{k}_i$ defining the local easy-axis direction [Fig. 8(b)].

Although the discretization shown in the figure may be viewed in purely mathematical terms, that is not always done. Indeed, it is quite common in practice to associate each element with a structural component of the sample, such as a grain of the magnetic film. Each element then represents in a sense, a certain typical grain of the sample. In that case, elements having special shapes (rectangular parallelepipeds, hexagons, spheres etc.), and which are not necessarily touching as in Fig. 8, may be used, in order to reflect the appropriate microstructure of the film. Finite elements may also be employed to model samples that have complicated shapes (22).

To proceed further with our example, we need to find appropriate numerical expressions for the effective fields acting on an element. The uniaxial magnetic anisotropy field, obtained by differentiating the energy expression, Eq. (17), is

$$\boldsymbol{H}_{\mathrm{k}i} = \frac{2K}{\mu_0 M_{\mathrm{s}}}(\hat{\boldsymbol{m}}_i \cdot \hat{\boldsymbol{k}}_i)\hat{\boldsymbol{k}}_i \tag{37}$$

To obtain the exchange field, we substitute a numerical form for the two-dimensional Laplacian $\nabla^2 \hat{m} = (4\,\hat{m} - \Sigma_j\, \hat{m_j})/h^2$ into the integrand of Eq. (21) and differentiate. This results in

$$\boldsymbol{H}_{\mathrm{x}i} = \frac{A}{M_{\mathrm{s}} h^2} \sum_j \hat{\boldsymbol{m}}_j \tag{38}$$

where the summation index $j$ runs over the four nearest neighbors of the element.

Since each volume element is assumed to be uniformly magnetized, it contains no volume charges ($\nabla \cdot \boldsymbol{M} = 0$), but instead, surface charges ($\boldsymbol{M} \cdot \hat{n}$) are induced on its bounding faces. The volume-averaged self-demagnetizing field acting on an element of the sample can be written as a summation (23):

$$\boldsymbol{H}_{\mathrm{d}i} = \frac{1}{V_i} \sum_k^n \sum_l^m \sum_{p=1}^6 G_{klp} \mathbf{M}_{kl} \cdot \hat{\boldsymbol{n}}_p, \tag{39}$$

where $V_i$ is the volume of the element and $M_{kl}$ is the magnetization vector of the array element ($k$,$l$). The summation index $p$ runs over the six bounding faces of an element, each of which bears the surface charge $\boldsymbol{M}_{kl} \cdot \hat{n_p}$. The coefficient $G_{klp}$ is the gradient of the *Green's function* of the problem for each bounding face. The Green's function is the potential functional for the problem that would result if all field sources were unit sources. It can be obtained in closed form for rectangular elements such as are used in our example (23).

Magnetostatic interactions are *long-range interactions*. The field due to a magnetic charge source drops off with distance $r$ from the source as $1/r^3$. This fact is not explicitly obvious from Eq. (10), but follows if we consider that according to Eq. (8), $\boldsymbol{H}_\mathrm{d}$ is obtained by differentiating a potential function that drops off as $1/r^2$. The volume $V$ of a three-dimensional object (not the essentially two-dimensional thin film of our example), on the other hand, grows as $r^3$. These reciprocal trends mean that the contributions of all points of the medium are significant and must be taken into account when computing $\boldsymbol{H}_\mathrm{d}$ for three-dimensional media. For two-dimensional media, however, volume varies as $r^2$, so that the contribution of a source point to $\boldsymbol{H}_\mathrm{d}$ now drops off as $1/r$. In this case a *truncation region* may be defined around a target field point, outside of which the contribution of the field sources to the demagnetizing field are negligible.

The system equation for the direct determination of demagnetizing fields, written for the $N$ discrete points of the medium, can be expressed in matrix form as follows:

$$\vec{H}_\mathrm{D} = \vec{D} \cdot \vec{Q} \qquad (40)$$

where $\vec{H}_D$ is an $N \times 1$ matrix of demagnetizing fields, $\vec{D}$ is the *demagnetization matrix* of dimension $N \times N$, and $\vec{Q}$ is a $1 \times N$ matrix of source terms. The elements of $\vec{D}$ are the derivatives of the Green's function of the problem. Their specific forms depend on the nature of the source entities, which may be volume charges, surface charges, line charges, or dipoles, depending on the formulation of the problem. In *deterministic* calculation methods, the elements of $\vec{D}$ depend on the geometry of the medium and remain unchanged throughout the calculation. They may therefore be precomputed and stored once at the start of the calculation, and then retrieved and reused many times in calculating $\vec{H}_D$. Typically, in such cases, certain symmetries in the geometry of the media element array permit some economization in the storage of elements of $\vec{D}$. In *adaptive methods* the size and the expressions for the elements of $\vec{D}$ change continually.

The direct use of Eq. (40) requires an $O(N^2)$ computational effort. This can be seen from our example expressed by Eq. (39). The order of evaluation of this equation is determined by the two outer summations and is equal to $N$ (the inner sum is not considered, as it represents a fixed operation on the faces of an element). Evaluating Eq. (39) for all $N$ elements of the medium results in an $O(N^2)$ calculation. As explained previously, the contribution of source points drops off as $1/r^2$ in thin films, and the number of terms in calculating $\vec{H}_D$ may therefore be reduced by truncation. This reduces the dimension of the demagnetization matrix $\vec{D}$ to $N \times M'$ and that of $\vec{Q}$ to $1 \times M'$, where $M' < N$. Reference 24 describes a hybrid truncation method, in which contributions of points within a certain distance from the point where $\boldsymbol{H}_\mathrm{d}$ is being evaluated are calculated exactly, and the effect of the remainder of the medium is approximated by *mean fields*.

Equation (40) can also be solved by means of intermediate transformations of the equation, as is the case with using the fast Fourier transform (*FFT*) method (Ref. 10, Chap. 9). The description of an adaptive method that is based on fast magnetic multipole expansions can be found in Ref. 25. Both the FFT and fast multipole expansion methods are $O(N \log N)$. Significant speeding up of calculation [to $O(\log N)$] has been reported in the literature, in a technique that formulates the calculation algorithm in a way that takes advantage of the multiprocessing capabilities of massively parallel computers (26).

We add the fields given by Eqs. (37, 38, 39, 40) to the external field $\boldsymbol{H}_0$ $(x, y)$ to obtain the total effective fields acting on the elements. If we now write the *LL* equation [Eq. (31)], for each element, we end up with a system of $N$ differential equations describing the magnetization of the system. These equations are to be integrated in order to calculate the magnetization response of the film. The equations are coupled to each other through the dependence of the effective fields on the magnetization of the medium. This system is integrated self-consistently over several time steps, using any of the standard iteration methods for integrating a system of equations, which are readily available in advanced numerical analysis texts. During the first iteration, the system is integrated over a small time increment $\Delta t_1$. This produces a new magnetization state of the film, evolved from the initial state. This new state is used to recalculate effective fields, which are in turn used to

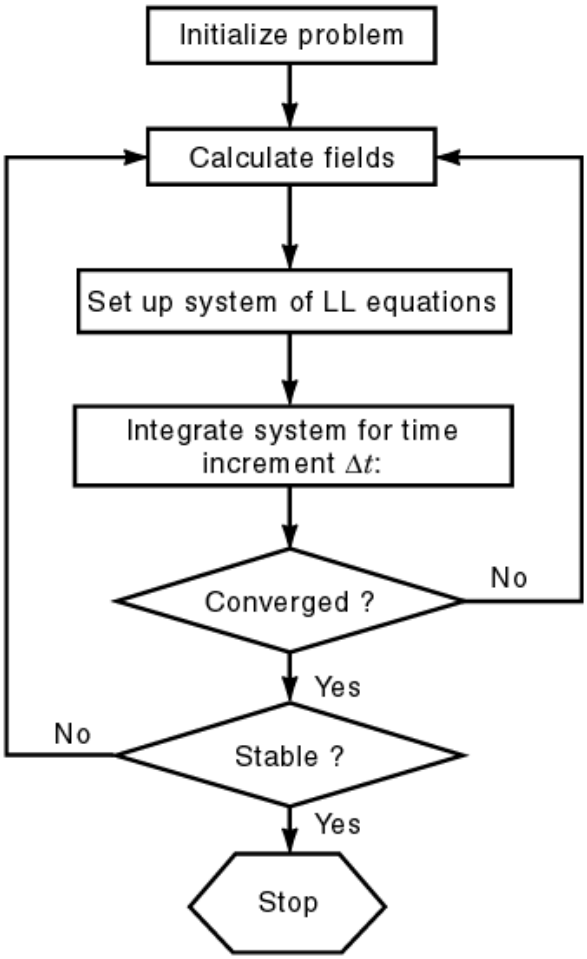


**Fig. 9.** Flow diagram of calculation algorithm for numerical micromagnetics example discussed in text.

update the system of differential equations, which are again integrated through a new time step $\Delta t_2$. This procedure is repeated several times until the equilibrium condition, Eq. (27), is satisfied. This happens when the torque per unit volume becomes everywhere less than some specified tolerance (usually a small positive number). The equilibrium state is tested for stability by randomly perturbing it and continuing the calculation. Stability is confirmed if the magnetic state rerelaxes back to the equilibrium state within a specified angular tolerance.

The calculation procedure described above is summarized in the flow diagram of Fig. 9. The time steps in the iteration must be chosen carefully so that no equilibrium state is overlooked. The physical total time to attain equilibrium is equal to the sum of the time steps used in the iteration ($\Sigma_l \Delta t_l$).

There are many factors that need to be taken into account to ensure accurate solutions to numerical micromagnetic problems. The interested reader may obtain information on continuing discussions and modern insights on these issues from the World-Wide Web site http://www.ctcms.nist.gov/~rdm/toc.html.

## ACKNOWLEDGMENT

The author gratefully acknowledges the valuable suggestions of the anonymous reviewers of this article that have been included as part of the text.

## BIBLIOGRAPHY

1. J. C. Maxwell *Treatise on Electricity and Magnetism*, 3rd ed., Oxford: Oxford Univ. Press, 1891.
2. W. F. Brown Jr. *Magnetostatic Principles in Ferromagnetism*, New York: North-Holland, 1963.
3. C. Kittel Physical theory of ferromagnetic domains, *Rev. Mod. Phys.*, **21**: 541–583, 1949.
4. E. Della Torre *Magnetic Hysteresis*, New York: IEEE Press, 1999.
5. J. C. Mallinson On damped gyromagnetic precession, *IEEE Trans. Magn.*, **MAG-23**, 2003–2004, 1987.
6. E. C. Stoner E. P. Wohlfarth A mechanism of magnetic hysteresis in heterogeneous alloys, *Phil. Trans. Roy. Soc. (London)*, **A240**: 599, 1948.
7. Y. D. Yan E. Della Torre Modeling elongated fine ferromagnetic particles, *J. Appl. Phys.*, **64**: 320–327, 1989.
8. J.-G. Zhu Micromagnetics of thin-film media, in C. D. Mee and E. D. Daniel (eds.), *Magnetic Recording Technology*, 2nd ed., McGraw-Hill, 1995.
9. H. N. Bertram *Theory of Magnetic Recording*, Cambridge, UK: Cambridge Univ. Press, 1994.
10. M. Mansuripur *The Physical Principles of Magneto-optic Recording*, Cambridge, UK: Cambridge Univ. Press, 1995.
11. S. Chikazumi S. H. Charap *Physics of Magnetism*, Malabar, FL: Krieger, 1978.
12. A. H. Morrish *The Physical Principles of Magnetism*, Malabar, FL: Krieger, 1983.
13. R. M. Bozorth *Ferromagnetism*, New York: IEEE Press, 1993.
14. J.O. Oti Y. K. Kim S. Suvarna A personal computer based semi-analytical micromagnetics design tool, *IEEE Trans. Magn.*, **33**, 4119–4121, 1997.
15. A. Aharoni Magnetostatic energy calculations, *IEEE Trans. Magn.*, **4**, 3539–3547, 1991; *Introduction to the Theory of Ferromagnetism*, Oxford, UK: Oxford Science, 1996.
16. W. K. Westmijze Studies on magnetic recording, *Philips Res. Rep.*, no. 8, p. 161–183, 1953.
17. C. Kittel *Introduction to Solid State Physics*, 5th ed., New York: Wiley, 1976, Chap. 15.
18. A. Hubert R. Schafer *Magnetic Domains*, New York: Springer-Verlag, 1998.
19. R. Moskowitz E. Della Torre Theoretical aspects of demagnetization tensors, *IEEE Trans. Magn.*, **MAG-2**(4), 739–744, 1966
20. H. Goldstein *Classical Mechanics*, Reading, MA: Addison-Wesley, 1981, Chap. 1.
21. M. Prutton *Thin Ferromagnetic Films*, Washington: Buttherworth, 1964, pp. 54–62.
22. T. R. Koehler Hybrid FEM–BEM method for fast micromagnetic calculations, *Physica B*, **223**: 302–307, 1997.
23. M. E. Schabes H. N. Bertram Magnetostatic interaction fields for a three-dimensional array of ferromagnetic cubes, *IEEE Trans. Magn.*, **MAG-23**: 3882–3888, 1987.
24. J. J. Miles B. K. Middleton A hierarchical micromagnetic model of longitudinal thin film recording media, *J. Magn. Magn. Mater.*, **95**, 99–106, 1991.
25. J. L. Blue M. R. Sheinfein Using multipoles decreases computation time for magnetostatic self-energy, *IEEE Trans. Magn.*, **27**, 4778–4780, 1991.
26. R. Giles P. S. Alexopoulous M. Mansuripur Micromagnetics of thin-film cobalt-based media for magnetic recording, *Comput. Phys.*, **6**, 53–70, 1992.

## READING LIST

J. O. Oti A micromagnetic model of dual-layer magnetic recording thin films, *IEEE Trans. Magn.*, **29**, 1265, 1993.

JOHN O. OTI
Euxine Technologies